water

MDPI

Article

Sea-Level Rise and Shoreline Changes Along an Open Sandy Coast: Case Study of Gulf of Taranto, Italy

Giovanni Scardino [1], François Sabatier [2], Giovanni Scicchitano [3], Arcangelo Piscitelli [4], Maurilio Milella [4], Antonio Vecchio [5,6], Marco Anzidei [7] and Giuseppe Mastronuzzi [1,*]

1 Dipartimento di Scienze della Terra e Geoambientali, Università degli Studi di Bari Aldo Moro, 70121 Bari, Italy; giovanni.scardino@uniba.it
2 Aix-Marseille Univ, CNRS, IRD, Coll de France, CEREGE, 13545 Aix en Provence, France; sabatier@cerege.fr
3 Studio Geologi Associati TST, 95045 Misterbianco Catania, Italy; scicchitano@studiogeologitst.com
4 Environmental Surveys s.r.l. Spin Off c/o Università degli Studi di Bari, 74121 Taranto, Italy; arcangelopiscitelli@ensu.it (A.P.); mauriliomilella@ensu.it (M.M.)
5 Radboud Radio Lab, Department of Astrophysics/IMAPP, Radboud University, 6500GL Nijmegen, The Netherlands; A.Vecchio@astro.ru.nl
6 Lesia Observatoire de Paris, PSL Research University, Université de Paris, 92195 Meudon, France
7 Istituto Nazionale di Geofisica e Vulcanologia, 00143 Rome, Italy; marco.anzidei@ingv.it
* Correspondence: giuseppe.mastronuzzi@uniba.it; Tel.: +39-080-544-2634

Received: 5 April 2020; Accepted: 13 May 2020; Published: 15 May 2020

Abstract: The dynamics of the sandy coast between Castellaneta and Taranto (Southern Italy) has been influenced by many natural and anthropogenic factors, resulting in significant changes in the coastal system over the last century. The interactions between vertical components of sea-level changes and horizontal components of the sedimentary budget, in combination with anthropogenic impact, have resulted in different erosion and accretion phases in the past years. Local isostatic, eustatic, and vertical tectonic movements, together with sedimentary budget changes, must be considered in order to predict the shoreline evolution and future marine submersion. In this study, all morpho-topographic data available for the Gulf of Taranto, in combination with Vertical Land Movements and sea-level rise trends, were considered by assessing the local evolution of the coastal trend as well as the future marine submersion. Based on the predicted spatial and temporal coastal changes, a new predictive model of submersion was developed to support coastal management in sea-level rise conditions over the next decades. After that, a multi-temporal mathematical model of coastal submersion was implemented in a Matlab environment. Finally, the effects of the relative sea-level rise on the coastal surface prone to submersion, according to the Intergovernmental Panel on Climate Change Assessment Reports (AR) 5 Representative Concentration Pathways (RCP) 2.6 and RCP 8.5 scenarios, were evaluated up to 2100.

Keywords: sea-level rise; coastal dynamics; erosion; accretion; submersion

1. Introduction

In recent years, the behavior of the Mediterranean coasts in relation to shoreline migration, as a consequence of the changes in the local sedimentary budget (e.g., [1–5]), and to the sea-level rise (e.g., [6–10]), has been of great interest. Currently, the sea-level change observed along the coasts depends on the sum of eustatic, steric, isostatic, and tectonic factors [11,12]. These factors, which prevail along the vertical direction, have been used to evaluate the submersion surfaces (e.g., [2,13–20]) for different sea-level rise scenarios for 2100 linked to climate change [21–27].

On a global scale, satellite altimetry revealed the absolute sea-level variations relative to the reference ellipsoid, showing a sea-level rise of 3.3 mm/year (NASA Goddard Space Flight Center data).

In the Mediterranean basin, however, tide gauge records revealed the sea-level height to the land upon which benchmarks are grounded, and a sea-level rise of 1.8 mm/year in the last century [28,29]. Sea level is expected to be 500–1400 mm higher than present by 2100 AD [21,22,27,30]. According to Church et al. [23,24] and the Intergovernmental Panel on Climate Change (IPCC) scenarios [25–27] during the 21st century, it is very likely that the global mean sea-level rise will exceed values observed in the last three decades, increasing up to 8–16 mm/year during 2081–2100.

1.1. Local Sea-Level Changes

Sea-level records in the Mediterranean over the last century show a sea-level variability depending on the location of the individual stations [28,29,31,32]. Rates vary in accordance with the length of the records, the local Vertical Land Movements (VLM), as well as the changes in atmospheric dynamics. In Antonioli et al. [33], the tide gauge data analyzed for the time span 2000–2013 at given localities along the Italian coasts, show sea-level rates ranging from 3.9 ± 0.2 mm/year (Ancona, Adriatic Sea) to 6.8 ± 0.1 mm/year (Cagliari, Tyrrhenian Sea), up to as much as 10.7 mm/year (Venice, Adriatic Sea). This is due to the decadal sea-level variability. Vecchio et al. [31] analyzed a set of long sea-level recordings (>60 years) for the northern Adriatic Sea, and estimated rates of around 1.2 mm/yr. However, at the subsiding tidal station of Venice Punta della Salute (Venice), rates reached up to 2.4 mm/year. In the Italian peninsula, as on other coasts of the Mediterranean and beyond, sea-level data show the occurrence of a continuous sea-level rise over the last decades compared to the previous centuries. Based on these rates, together with the contribution of VLM and the climatic scenarios reported in the IPCC Assessment Reports (AR) 5, and Representative Concentration Pathway (RCP) 8.5, a relative sea-level rise of approximately 0.8 m is expected by 2100 in the northern Adriatic Sea, and about 0.6 m for the Gulfs of Cagliari and Taranto. However, several authors [21,22,30,34] predict a more severe global sea-level rise of up to about 2 m by 2100, applying regional climate models [32] and a variety of statistical approaches in combination with VLM [31]. The latter value would cause a dramatic submersion of global coastal areas, and would affect human settlements, industrial and commercial facilities, archaeological and cultural heritage sites, and natural areas. Sea-level rise warnings and coastal hazards have been issued globally [35], as well as in Italy [2,16–20,33,36]. In addition, human activities may produce land subsidence due to compaction or extraction of fluids from the alluvial sequences, determining local subsidence up to several mm/yr, thereby increasing local sea-level rise [2,37–40].

1.2. Coastal Behavior in Function of Sea-Level Rise

While many studies have focused on the sea-level rise, few have described its effects along the coasts. This may be due to the difficult approach to sedimentary coastal budget and its dynamics, which only the common Bruun rule model [41] can help overcome. Currently, the Italian coast is influenced by a decrease in the sedimentary input owing to natural and anthropogenic conditions, e.g., dams and hydrological adjustments, changes in vegetation cover and climate, erosional/depositional capacity of the rivers, defense interventions along the coastal stretches. These conditions are making the coastal system changes, caused by atmosphere dynamics and rising sea level [31,33,38], difficult to assess. Thus, only a fallacious answer may explain how coastal landscapes respond to the landform re-organization during an accelerated sea-level rise. This is especially the case for those tracts, such as sedimentary coasts, that may undergo rapid morphological changes in river drainage basins in order to attain new equilibrium profiles [9,10,42,43]. Predicting a future scenario for every coast set within Valentin's milestone diagram [44] (Figure 1) is not an easy task. Hence, many areas along the Mediterranean coasts will be susceptible to submersion by future sea-level rise and severe flooding [20,29,31].

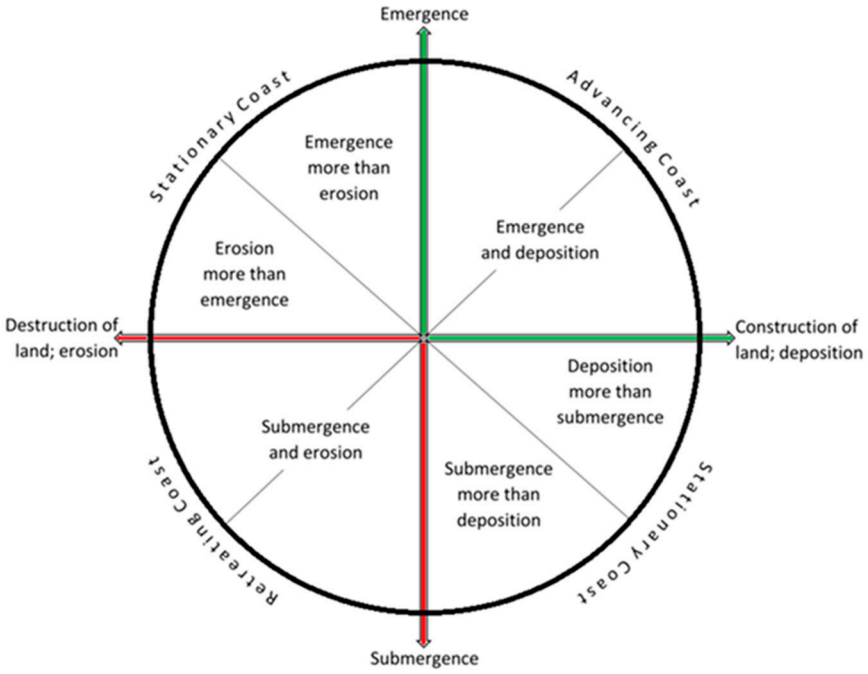

Figure 1. Valentin Diagram [44] which defines the changes in the shoreline in combination with relative sea-level rise.

1.3. Objective

Projected sea-level rises could determine significant future surface loss on the low-lying coastal regions in the Mediterranean basin.

Furthermore, sea-level rise could cause permanent surface submersions in many Mediterranean coastal areas. Thus, it is important to assess the surfaces that could be submerged at any given moment of the future [2,19,33,45].

This paper proposes a new mathematical model for predicting possible submersion scenarios as the one developed for the area of the northern coast of the Gulf of Taranto in Southern Italy. It will consider the changes in both the vertical sea-level components and the horizontal shoreline components, beginning from the past articulation and behavior of the mobile coastal systems. To highlight the coastal response in function of sea-level rise, knowledge of coastal changes and decadal sea-level changes will be reviewed, while, to assess the coastal response linked to the sea-level rise, various existing models will be considered e.g., [9,41,43,46,47].

The aim of this paper is to develop a submersion model of the relative sea-level rise scenario estimated for the coastal plain on the Gulf of Taranto by 2100.

2. Geomorphological Setting

The Metaponto coastal plain covers most of the northern coast of the Gulf of Taranto. The plain takes its name from the ancient Magna Grecia colony of Metapontum, whose remains are still standing today. It stretches NNE to SSW from the Taranto area, and runs along the foredeep of the Bradanic Trough, up to the area of Roseto Capo Spulico, at the eastern border of the Apennine Chain (Figure 2a).

The coastal plain is the result of the sedimentary body accumulated during the last 7 kyear (10^3 years) on the local basement. It was shaped by marine processes which produced a ravinement surface at the base of an old cliff. This coastal plain was conditioned by the interplay between the eustatic sea-level rise during the post Last Glacial Maximum (LGM) transgression and the regional uplift [48,49]. The coastal plain has been heavily supplied by siliciclastic sediments discharged by the main rivers crossing the Apennine chain (Agri, Sinni, Cavone, Bradano, and Basento Rivers). It is

composed of quartz, polymineralic lithics and bioclasts [48,49] which are distributed SSW to NNE by the longshore drift.

The landscape of the coastal area adapted to the ice-sheet melting after the Last Glacial Maximum (LGM) of 18 kyear (e.g., [7,49–54]).

In particular, these main phases can be recognized:

- Marine Isotope Stage (MIS) 2—Last Glacial Maximum (LGM): sea-level stand at about 120 m below the present sea level and deep engravings on the coastal wedge up to the shelf break
- 20-6/7 kyear: sea-level transgression with a rate of 8 mm/year and re-shaping of incised valleys along the Gulf of Taranto
- from 6/7 kyear to the second half of twentieth century: sea-level rise allowing the growth of the coastal plain and beach-dune system progradation conditioned by NE longshore drift.

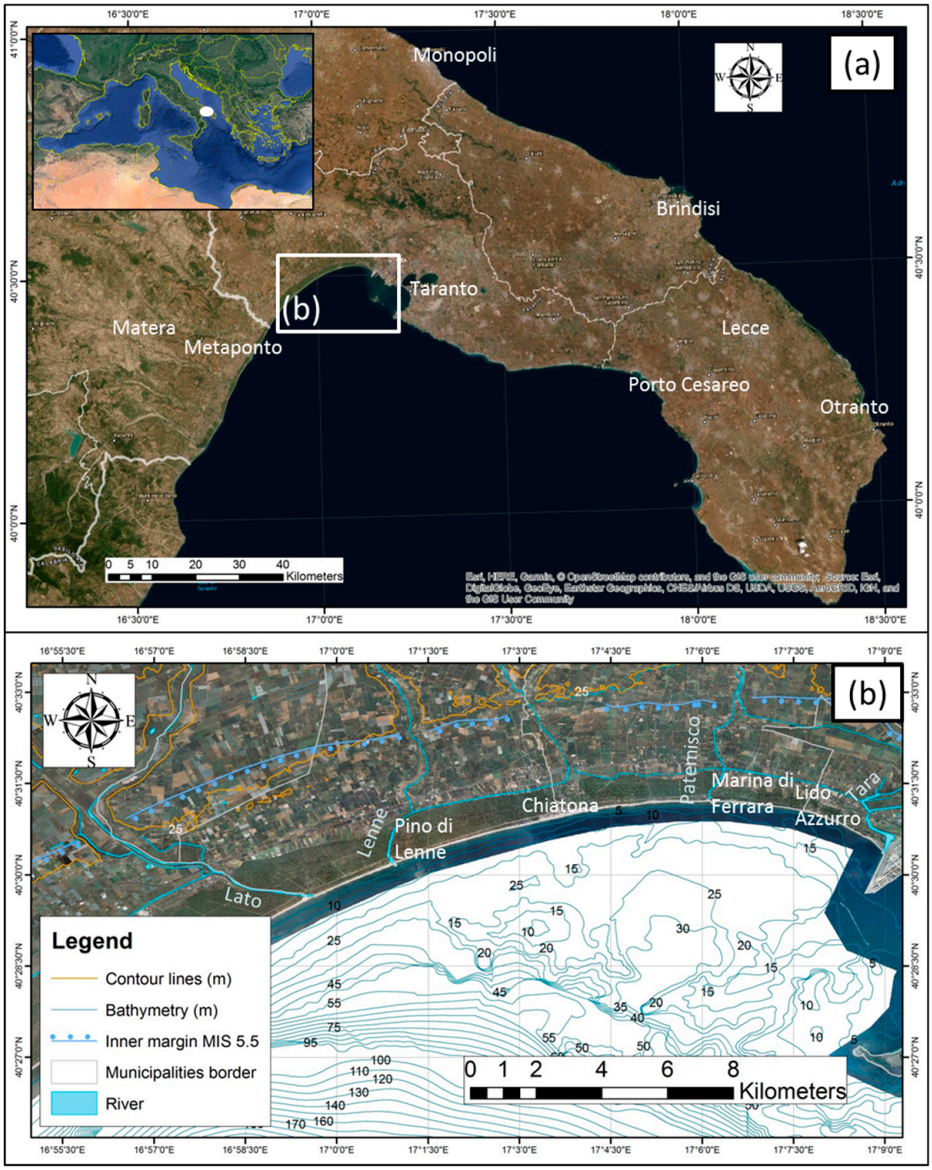

Figure 2. The study area of the Apulia region (Southern Italy): (**a**) the coastal plain of the Gulf of Taranto, Northeastern to Southwestern trending, highlighted by the white box and (**b**) the coastal stretch extending between Castellaneta and Taranto.

The Metaponto plain is bordered landward by a progradated mobile coastal system [55,56] consisting of a series of polyphasic, quasi-parallels dune belts, extending more than 1000 m inland

and characterized by an altitude ranging between 8 and 17 m [56,57] (Figure 2b). The dune belts are characterized by an accentuated lateral continuity, and are largely colonized by the "Macchia Mediterranea", e.g., vegetation assemblages stabilizing the innermost dunes. The back-dune areas are characterized by low-lands that, in the past, hosted a lagoon, reclaimed at the beginning of the twentieth century. A primary dune belt is bordered and supplied by a medium/fine sandy beach with a gently sloping profile, currently undergoing strong erosion.

The entire coastal area was in progradation up to the late 1950s. In many areas, dunes show strong evidence of significant shoreline retreat, highlighted by cliffs shaped in the dune deposits (Figure 3). This retreat has been induced by a negative sedimentary input as a result of: (i) the anthropogenic modification of the river basin catchments with the realization of large dams and hydrological works during the second half of the twentieth century and, (ii) more recently, the conditioning of the longshore drifting due to the building of some touristic harbors and coastal defenses ([58] and references therein).

This mobile coastal system is characterized by an intermediate surf zone domain between reflective and dissipative hydrodynamic regimes, producing marked changes of nearshore sea-floor features [4,49]. Originally, the studied mobile coastal system was characterized by an intermediate morpho-hydrodynamic state, with rhythmic bars located where wave interactions cancel net bottom stress.

At present, these bars act as natural breakwaters, reducing wave energy in the proximity of the shoreline. This influences the currents that allow sediment movement along the entire littoral zone up to a seaward annual closure depth equal to 7.3 m [59].

The study area corresponds to the easternmost part of the plain, stretching between Castellaneta and Taranto. As in the rest of the plain, the mobile coastal system is characterized by well-defined beach-dune belt-back dune areas; several orders of parallel dune belts with elevations of up to about 15 m above sea level (a.s.l.), crowned by a backshore with widths ranging from 25 to 40 m and a foreshore width of up to 15 m. Four short rivers, the Lato, Lenne, Patemisco, and Tara, are mainly supplied by karst aquifers from East to West across the coastal plain without significant sediment supply to the mobile coastal system.

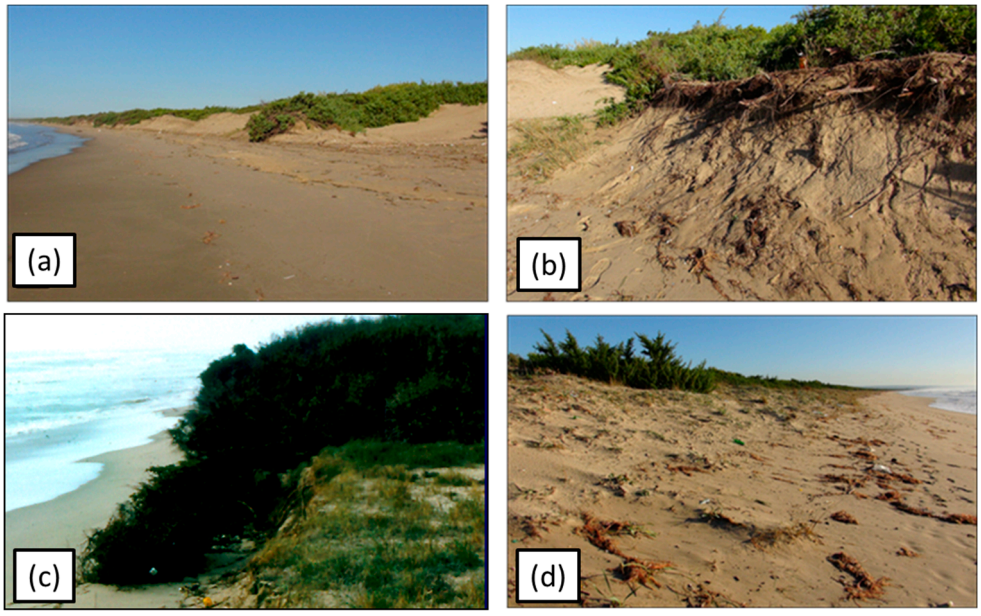

Figure 3. Dune erosion observed in the Gulf of Taranto: (**a**) The Lido Azzurro coast was flooded by storm events in the winter of 2018. Note the erosion of the dune belt; (**b**) a detail of the Lido Azzurro coast with the eroded dune and the exposed plant roots; (**c**) flooding and erosion of a secondary dune in the proximity of the Lato river mouth; and (**d**) dune belt erosion of the Chiatona beach.

3. Methodology

3.1. Data

3.1.1. Tectonics and Isostasy

The Taranto area is characterized by a weak vertical tectonic uplift of the Late Pleistocene and the Holocene. This can be inferred by the elevation of the inner margin of the Marine Isotope Stage (MIS) 5.5 deposits in the Taranto area at 23 m a.s.l. and up to 40 m between Metaponto and Policoro (e.g., [52–54,60–62]).

The different altitudes of the MIS 5.5 terrace indicate decreasing values of long-term uplift rates, from West to East, along the Gulf of Taranto, from 0.39 mm/year close to the Apennine Chain, to 0.26 mm/year in the Taranto area [40,52].

To evaluate the isostatic components, the Lambeck et al. models [11,13] were applied. They consider three-layers, an elastic lithospheric thickness of 110 km, an upper mantle viscosity of 3×10^{20} Pa·s and a lower mantle viscosity of 3×10^{22} Pa·s, providing a rate of the Vertical Land Movement at about 0.45 mm/year in the Gulf of Taranto.

An Interferometric Synthetic Aperture Radar (InSAR) analysis [63] did not show evidence of anthropogenic-induced displacement in the Taranto area. This reveals the general tectonic stability in the NE end of the gulf and a very slight subsidence trend in the northern part of the City of Taranto. To assess the current rates of VLM along the coastal zones of the Mediterranean region, a continuous GPS (cGPS) dataset, analyzed in the frame of the SAVEMEDCOASTS Project (www.savemedcoasts.eu [64]), was used. This study focuses on the uplift velocity estimated at the cGPS station of MMET (Matera METaponto) which falls within the investigated area located in Metaponto (Matera, Southern Italy). This station is managed by the Italian Space Agency (ASI/CGS) and is integrated in the Rete Integrata Nazionale GNSS (RING) network (http://ring.gm.ingv.it/ [65]). Vertical GPS velocity has been determined in the IGb08 realization of the global ITRF08 absolute geocentric reference frame [31,64,66] providing an uplift of 0.29 ± 0.14 mm/year.

3.1.2. Tide and Sea-Level Trend

The current sea-level trend between Castellaneta and Taranto was obtained using sea-level data recorded by the Istituto Superiore per la Protezione e la Ricerca Ambientale (ISPRA), tidal station located at the Molo Sant'Eligio, in the Taranto harbor. Data were continuously recorded with a sampling rate of 10 min using an ultrasound transducer SIAP ± MICROS ID0710 (from 1999 to 2010, ISPRA, Taranto, Italy), and a radar sensor SIAP + MICROS TLR (from 2010 to 2020, ISPRA, Taranto, Italy). During the analysis, gaps and outliers were recognized and corrected to avoid artificial signals in the time series. The analysis highlighted a semidiurnal tidal range of 0.4 ± 0.1 m and a mean sea-level rise of 1.04 ± 0.5 mm/year in the time span 1999–2020 (20 years) (Figure 4). The tide gauges located along the Apulian coasts, managed by ISPRA and the Autorità di Bacino della Puglia (AdBP), have shown a continuous sea-level rise in the last two decades, with similar trends for Taranto (Figure 5).

3.1.3. Orthophoto and Satellite Images

Aerial orthophotos were obtained from the Istituto Geografico Militare (IGM), the Apulian Servizio d'Informazione Territoriale (SIT) of the Apulia Region, and the Ministero dell'Ambiente. Images were collected during the past 70 years (about 1947–2018). Satellite images were derived from WorldView2/3 (DigitalGlobe, Westminster, U.S.), RapidEye (Satellite Imaging Corporation, Canada, U.S.), and Declass1 satellites (USGS, U.S.) for the time span period 1961–2018 (Table S1, supplementary material).

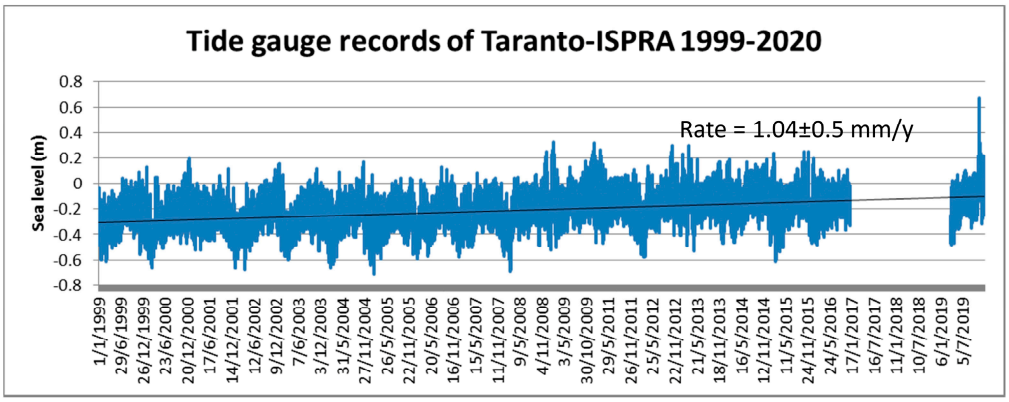

Figure 4. Sea-level time series for the Taranto station in the time span 1999–2020, recorded at a 10-minute sampling rate. The black line is the linear fit of the data that provide a sea-level rate of 1.04 ± 0.5 mm/year.

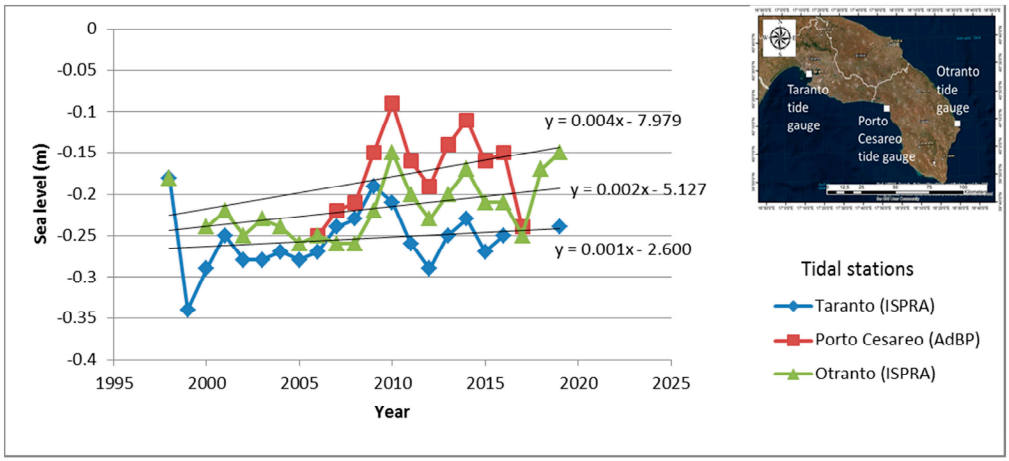

Figure 5. Annual mean sea-level records at the Taranto, Otranto, and Porto Cesareo tidal stations (retrieved from www.mareografico.it [67] and www.adb.puglia.it [68], ISPRA—Istituto Superiore per la Protezione e la Ricerca Ambientale and AdBP—Autorità di Bacino della Puglia).

From each image, the shoreline was extracted, the weather conditions at the time of acquisition were considered, and the barometric effects reduced, using the Theiler et al. method [69].

3.1.4. LIDAR and TLS

Laser Imaging Detection and Ranging (LIDAR) data were derived from the 2008–2009 surveys performed by the Ministero dell'Ambiente, at a resolution 2 × 2 m. In addition, Terrestrial Laser Scanner (TLS) surveys were performed at different times during the winter of 2018 by means of the Faro Focus X130 (Polo Scientifico Tecnologico Magna Grecia, Taranto, Italy), at a resolution of 2 cm. LIDAR and TLS data and Digital Elevation Models (DEMs) were combined to extract the shoreline configuration and the shore morpho-topography (Figure 6). For the considered coastal stretches, DEMs reveal a mean shoreface slope between 2 and 5 degrees which, in response to the tide amplitude, determines a daily horizontal shoreline displacement of 12.5 ± 3 m under a low hydrodynamic condition. A reference value to evaluate the shoreline rate changes was obtained by integrating long-term changes, detected by orthophotos and satellite images, with short-term changes detected by TLS data.

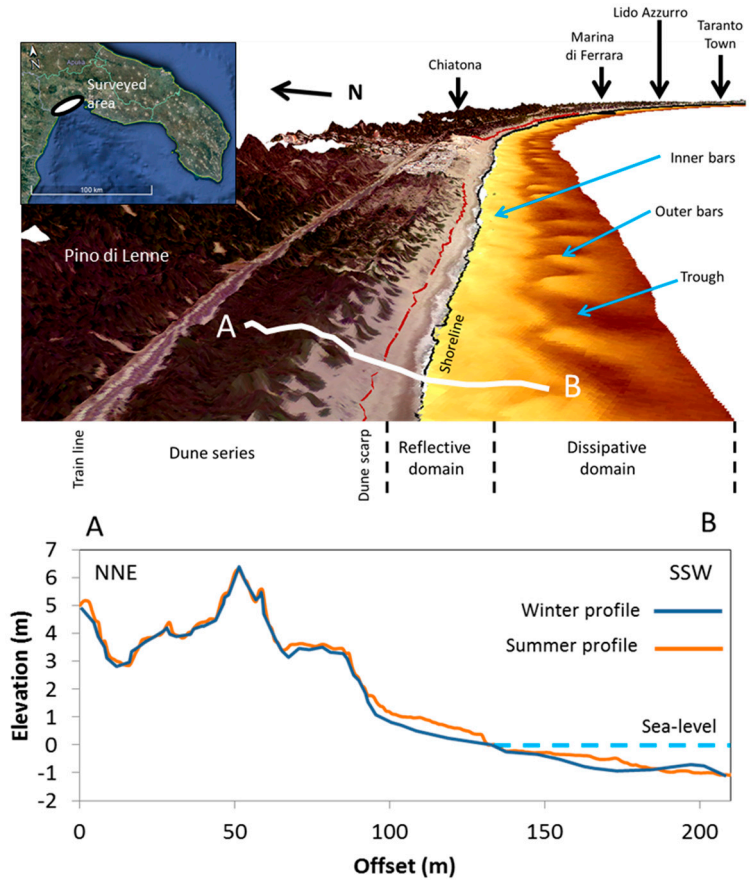

Figure 6. Morpho-topographic and morpho-bathymetric digital models obtained by direct surveys performed on the sandy coast stretching from the Castellaneta beach to the City of Taranto.

3.2. Data Processing

An analysis of the spatial and temporal changes in the Ionic littoral zone between Castellaneta and Taranto was performed by digitalizing all the shorelines via aerial photographs, orthophotos, satellite images, and LIDAR data available for that stretch of coast. They were collected for a medium-term analysis and integrated with TLS data acquired at different hours on different days. From all the collected images, the shorelines were digitalized in ArcGIS for each year. Digital Shoreline Analysis System (DSAS) tools were also used [69] in order to obtain the shoreline 1947 to 2018 changes. During the processing, uncertainty about the position of the shoreline had to be defined. The following factors were considered:

- Line drawing of the operator on the swash zone with an error range of ±3 m
- Weather conditions (tide excursion, atmospheric pressure, temperature, sea level, wind) at time of image acquisition with an error range of ±0.4 m
- Instrumental accuracy with an error range of 0.31–0.5 m
- Computer errors with an error range of ±0.1 m

For the entire stretch of the sandy coast, 345 transects (50 m spacing) were extracted perpendicularly to a reference baseline placed 50 m seaward. The distance between the baseline and each shoreline intersection point made it possible to obtain metric measurements and all shoreline change rates, expressed as meters of change along the transects per year. To determine the different behaviors of the sandy coastal stretches, these estimates were obtained for three different portions of the sandy coast, each in lateral continuity from West to East (Figure 7). For each time span, the minimum, maximum,

weighted average, and error range were evaluated. The choice of the weighted average is related to the density data for a given time range (Figures 8 and 9).

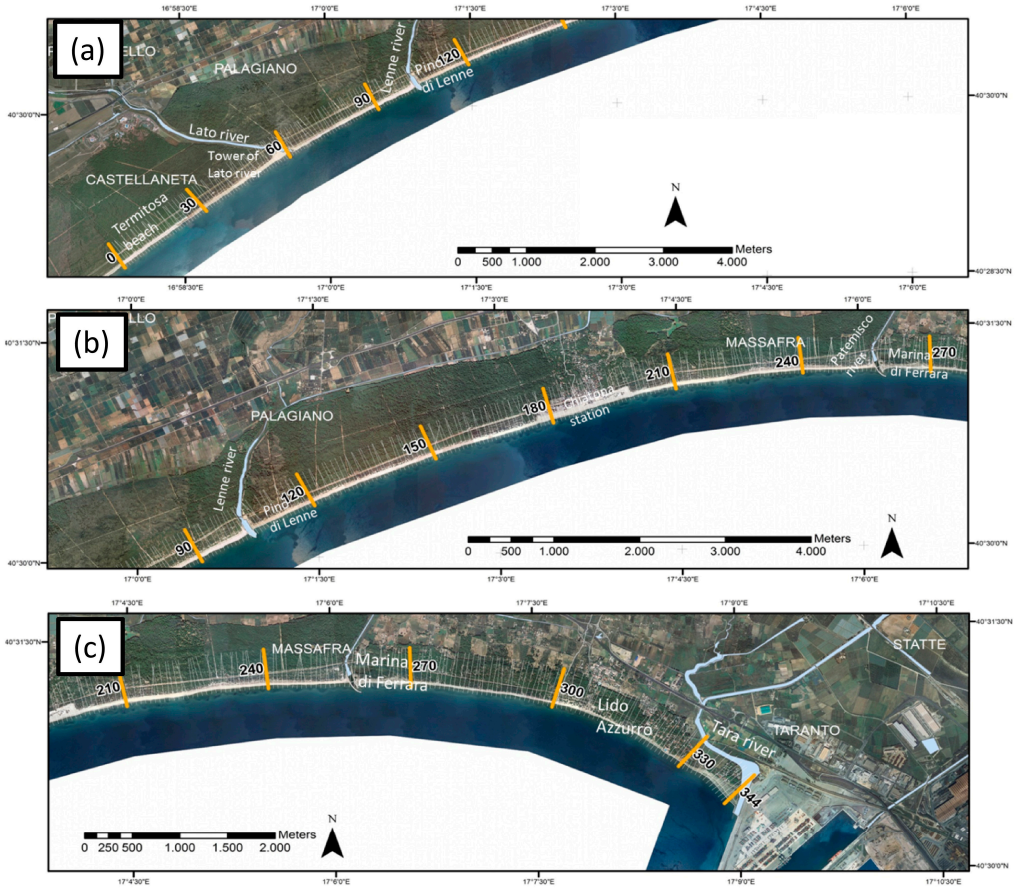

Figure 7. Coastal stretches analyzed in this study. Each transect is reported in the figures; (**a**) CS1 from the Pino di Lenne beach to the Castellaneta beach; (**b**) CS2 from the Marina di Ferrara beach to the Pino di Lenne beach; and (**c**) CS3 from the Tara River mouth to the Lido Azzurro beach.

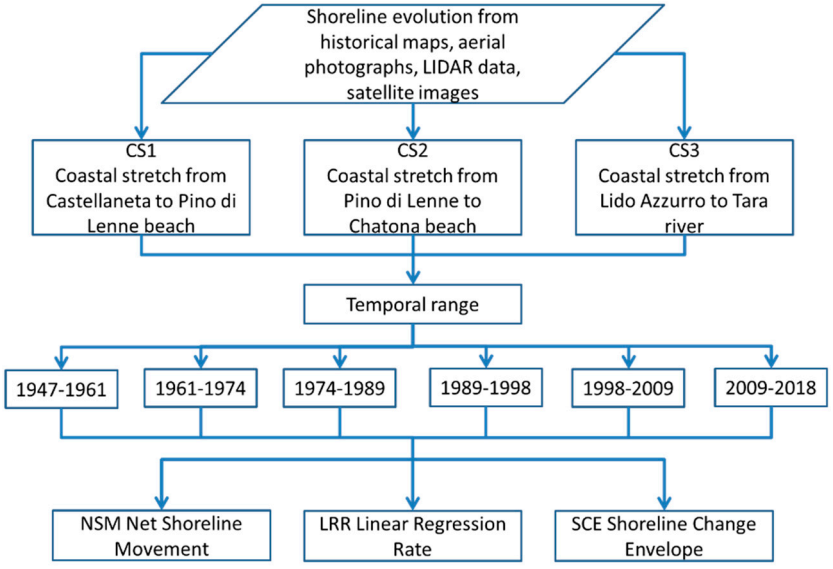

Figure 8. Flow chart of shoreline change analysis performed over different time spans using Digital Shoreline Analysis System (DSAS).

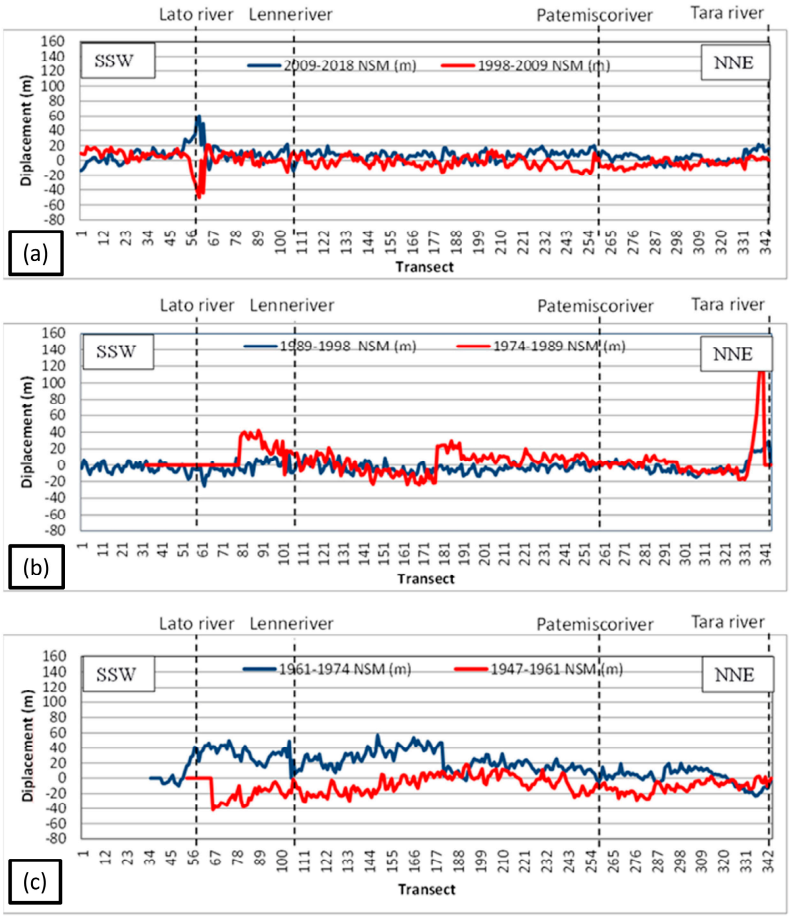

Figure 9. Net Shoreline Movement (NSM) for the study area: (**a**) NSM during the 2009–2018 and 1998–2009 time spans; (**b**) NSM during the 1989–1998 and 1974–1989 time spans; and (**c**) NSM during the 1947–1961 and 1961–1974 time spans.

3.3. Predictive Model of Submersion Surfaces Connected to Sea-Level Rise for 2100

Predicted coastal changes in response to sea-level rise may reflect a different behavior in function of the geomorphological elements of a sandy coast. These may determine three different scenarios: (i) a barrier erosion with dispersed sediments on the shoreface just above the wave base, as described by Bruun [41]; (ii) a rolling-over of the barrier, migrating onshore through mass relocation [43]; and (iii) an overstepping or in-place drowning in response to a fast sea-level rise with a complete submersion of the barrier.

A mathematical submersion model was implemented according to the concept that the 3D geometric shoreline displacement and subsequent migration of the intertidal zone are caused by a sea-level rise and horizontal shoreline movements. The development of a submersion model along a sandy coast requires knowledge of the following parameters: (i) sea-level trend; (ii) VLM rates, including isostatic adjustments; and (iii) shoreline erosion/accretion. The model was implemented mathematically in a Matlab environment by considering the components conditioning both the vertical and horizontal coastal displacements for the sea level and shoreline changes:

$$\Delta z = (v_{RSLR} \times 10^{-3}) \times \Delta t \pm \Delta z_{\ tide} \quad (1)$$

$$\Delta x = v_{LRR} \times \Delta t \times \cos \beta \quad (2)$$

$$\Delta y = v_{LRR} \times \Delta t \times \sin \beta \quad (3)$$

where:

Δz—relative sea-level rise (m)
v_{RSLR}—relative sea-level rate (mm/year)
Δt—prediction time span (year)
Δz_{tide}—tide amplitude (m)
Δx—longitude shoreline displacement (m)
Δy—latitude shoreline displacement (m)
v_{LRR}—shoreline rate changes (m/year)
β—normal shoreline angle (degrees).

The output provides all the points corresponding to the submersion surface predicted up to 2100, presented in a GIS-layer format with the xyz coordinates in world metric reference.

4. Results

4.1. Shoreline Changes

The multi-temporal analysis of the shoreline changes highlighted a marked erosion between 1947 and 1967, followed by a significant shoreline accretion up to 1998 (already shown by [48,49]) and, finally, another erosion period up to 2018. Important changes in the entire sandy coast were revealed, together with river mouth changes (Figure 10).

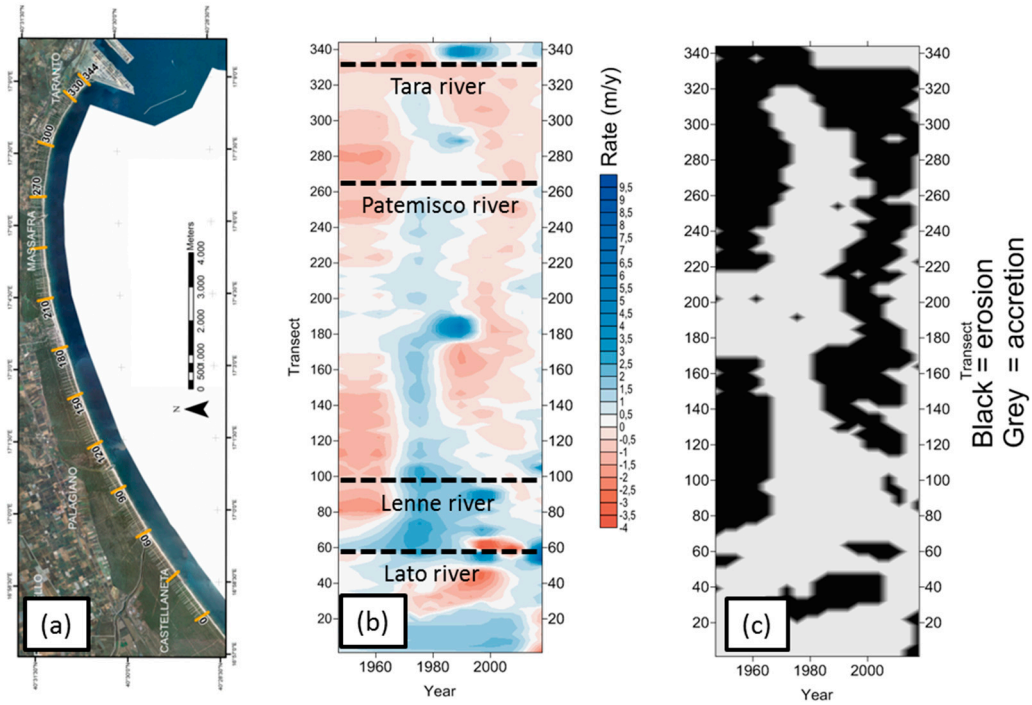

Figure 10. Shoreline evolution of the investigated sandy coast: (**a**) Map with transects; (**b**) shoreline change rates (red indicates the erosion, while blue, the accretion); and (**c**) shoreline changes: grey indicates the advancements, while black the retreats.

The first and most important event is connected to the shoreline accretion close to the Tara River. The 120 m accretion which occurred in 1987 was significant, and can be attributed to the construction of the Taranto Harbor (Figure 11).

The Patemisco River mouth showed a substantial modification in width during 1960, subsequent to the armored anthropogenic construction devised to deviate the longshore drift. In this area, a marked past change on the shoreline and dune (Figure 12) can be noted. In particular, the nearshore bar movements caused by wave diffraction may be observed (Figure 12e).

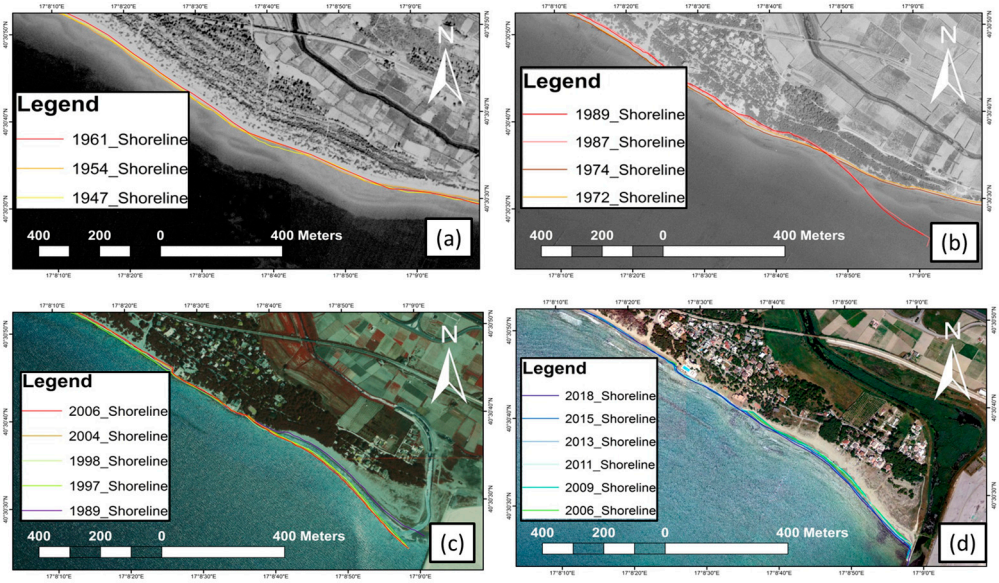

Figure 11. Shoreline changes close to the Tara River mouth: (**a**) 1954 basemap with 1947–1961 super-imposed shorelines; (**b**) 1974 basemap with 1972–1989 super-imposed shorelines; (**c**) 1989 basemap with 1989–2006 super-imposed shorelines; and (**d**) 2013 basemap with 2006–2018 super-imposed shorelines.

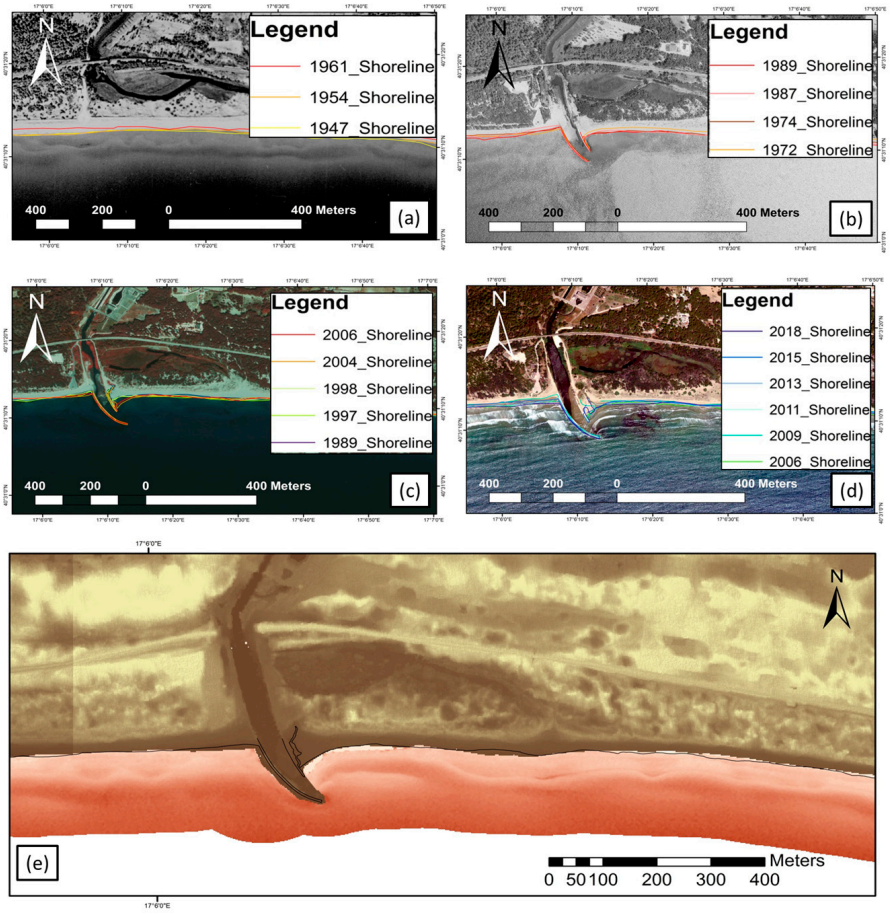

Figure 12. Shoreline changes close to the Patemisco River mouth: (**a**) 1954 basemap with 1947–1961 super-imposed shorelines; (**b**) 1974 basemap with 1972–1989 super-imposed shorelines; (**c**) 1989 basemap with 1989–2006 super-imposed shorelines; (**d**) 2013 basemap with 2006–2018 super-imposed shorelines; and (**e**) Laser Imaging Detection and Ranging of 2009 nearshore topography and morpho-bathymetry.

The Lenne River revealed different full-mouth events, marked by the building of dykes. The latter hinder transversal sediment transports and amplify sand accumulation near the river mouth during storm events (Figure 13). Compared to other rivers, the Lato River is less affected by anthropogenic contributions, and shows little accretion or variable mouth shape, connected to the sea-state regime and longshore currents (Figure 14).

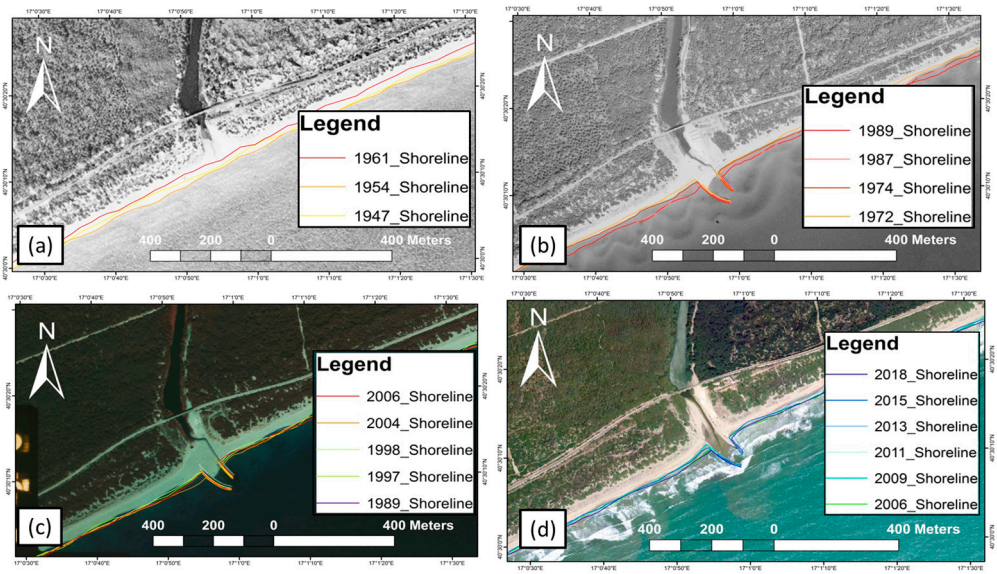

Figure 13. Shoreline changes close to the Lenne River mouth: (**a**) 1954 basemap with 1947–1961 super-imposed shorelines; (**b**) 1974 basemap with 1972–1989 super-imposed shorelines; (**c**) 1989 basemap with 1989–2006 super-imposed shorelines; and (**d**) 2013 basemap with 2006–2018 super-imposed shorelines.

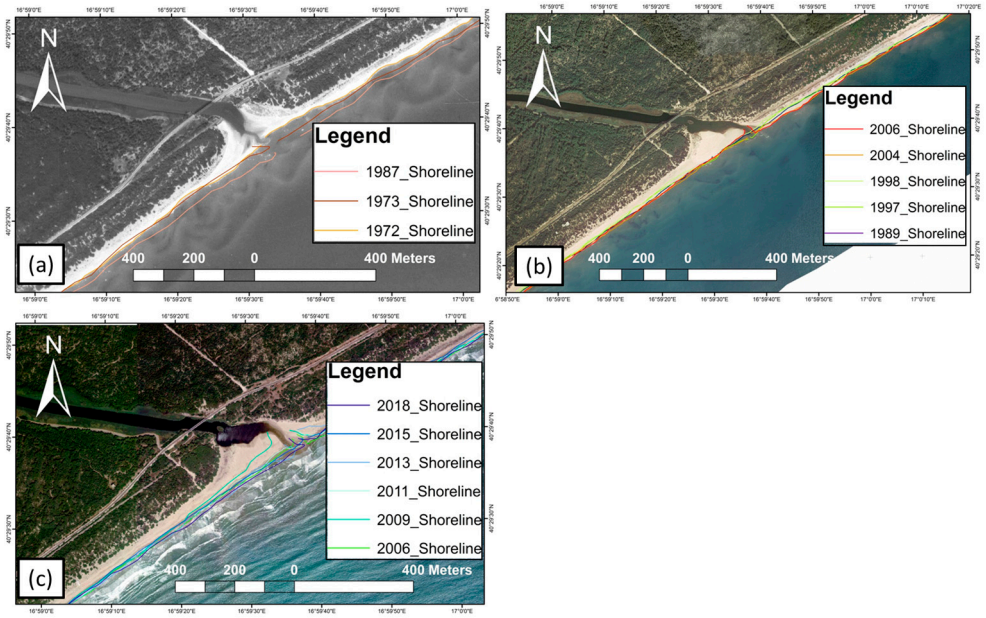

Figure 14. Shoreline changes close to the Lato River mouth; (**a**) 1972 basemap with 1972–1987 super-imposed shorelines; (**b**) 2006 basemap with 1989–2006 super-imposed shorelines; (**c**) 2013 basemap with 2006–2018 super-imposed shorelines.

A variable dynamic is recognizable along the Castellaneta beach, close to the Lato River. This is directly connected to the sea-state influence together with the behavior of the Lato River mouth in the past. Indeed, the hot spot values of the shoreline migration for the transects, corresponding to

the Lato River mouth (Figure 10), may be identified. During 1947 and up to 1961, a shoreline erosion trend of −0.38 ± 0.17 m/year occurred, with a maximum net movement of about 7.49 m. This was followed, in the subsequent years (1961–1987), by a shoreline accretion having the same maximum net movement.

From the Lenne River mouth, crossing the Pino di Lenne beach and Chiatona beach (Figures 2–6), a significant shoreline erosion rate of −0.42 ± 0.19 m/year occurred up to the 1970s. This was followed by a general accretion rate of 1.26 ± 0.66 m/year, occurring, in particular, in proximity to the Chiatona railway station, and to the numerous holiday resorts built along the coast. Subsequent sediment redistribution took place between the 1970s and the 2010s. Then, during the period 1990–2010, an erosion rate of −0.36 ± 0.18 m/year occurred.

During the mid-twentieth century (1950–1970), the shoreline change rate between the Marina di Ferrara and the Lido Azzurro highlighted the retreat of some portions of the dune systems, at a rate of −0.81 ± 0.36 m/year. Furthermore, with the construction of the Lido Azzurro holiday resort, an acceleration of this retreat occurred, showing that the current position of the shoreline corresponds to the position of the dune scarp in the 1970s. As of 1989, there has been an erosion rate of −0.23 ± 0.11 m/year, and, as of 1998, an erosion rate of −0.40 ± 0.13 m/year. On the contrary, the building of the breakwater structures in the Taranto harbor, together with the supply trend of the Tara River, changed the shoreline configuration dramatically during the 1970s–1990s.

4.2. Geomorphological Scenario for the Future

An analysis of the dune-beach system topography indicates geomorphological scenarios similar to those described by Davidson-Arnott [47], e.g., a sea-level rise corresponds to a shoreline retreat and beach/dune erosion as a result of the reduction in the sedimentary budget connected to a river transport decrease. A conceptual geomorphological model for the sea-level rise along the coast stretching between Castellaneta and Taranto was deduced by analyzing a sequence of aerial photos from 1947 to present, as well as by using direct surveys (Figure 15).

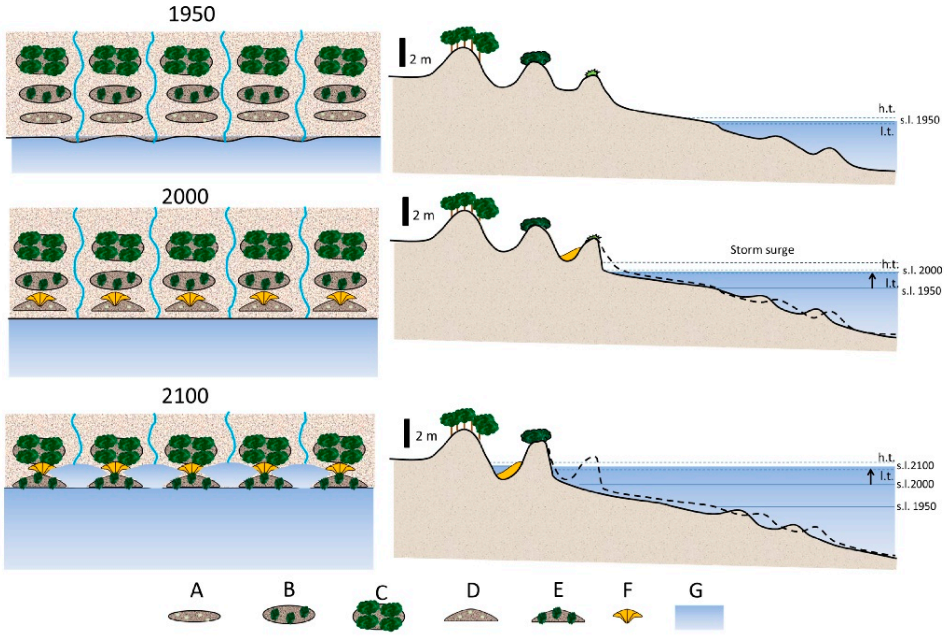

Figure 15. The conceptual model for coastal submersion in function of the mean sea-level rise, and changes in foreshore between high tide (h.t.) and low tide (l.t.). A—Primary Dune Ridge; B—Secondary Dune Ridge; C—Tertiary Dune Ridge; D—Eroding Primary Dune Ridge; E—Eroding Secondary Dune Ridge; F—Aeolian Sand Deposits; and G—Sea.

In the first half of the twentieth Century, a progradation of the mobile coastal system was observed [48,49,56,70] with a well-extended dune system up to 1 km landward stabilized by vegetation cover.

Between the 1950s and 2000s, two phases of coastal erosion were observed throughout the entire littoral area: sea-level rise and increase in the number of storm events, and a decrease in the amount of natural sedimentary nourishment coming from the land. A foredune erosion was observed, and the foredunes along the coastal stretches near the Lato River were completely destroyed. Furthermore, erosion of the secondary dunes was also observed. The building of holiday resorts in the area of the Chiatona and Lido Azzurro coastal stretches caused foredune leveling and increased vulnerability to effects of the sea-level rise.

Within the framework of an increase in the speed of the sea-level rise up to 2100 [27,31], together with an increase in storm intensity [32], the coasts around the Gulf of Taranto could be subjected to a shoreline regression, coupled with a partial foredune erosion and subsequent marine ingressions through river mouths, not to mention submersion of low-lands behind the dune ridge.

5. Discussion

5.1. Simulating the Impact of a Rising Sea Level—A Difficult Methodology

The sandy coast of the Gulf of Taranto is characterized by a complex dynamics system, making the exact shoreline position very difficult to assess. First of all, it can be assumed that if the coast is considered to be in a steady-state, with no significant sediment movements, the shoreline migration should be subjected to only vertical displacements of the relative sea level. By considering the sea-level rise recorded at the Taranto-ISPRA station, different horizontal displacement rates, in function of the coastal slopes (Figure 16), can be derived. Second of all, geometric horizontal shoreline movements due to sea-level rise were subtracted from the observed shoreline movements in order to obtain effective shoreline change (Table 1) and to apply a correct value of horizontal displacement for the three coastal slopes considered in Figure 7.

The observed shoreline movements show very different results from the geometric horizontal migrations induced by a sea-level rise (Table 1 and Figure 10). According to this methodology, the sea-level contribution to the shoreline retreat is lower than 10%. Factors contributing to the shoreline retreat, other than the sea-level rise, such as the gradient of longshore sediment transport, negative sediment input due to dam and hydrological adjustments or construction of holiday resorts along the coast, were all considered. Albeit the investigated area is part of a bay, the beach dynamics have most probably been wave-dominated up to now, but increasing sea levels could modify this behavior.

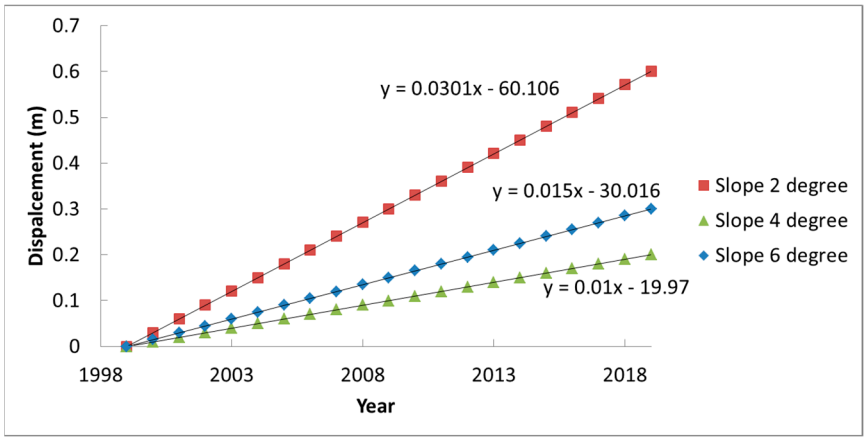

Figure 16. Horizontal displacements obtained following a geometric steady-state approach: sea-level rise determines a landward shoreline movement without accretion, where the shoreline rate change is dependent only on the coastal slope.

Table 1. Effective shoreline rate changes between 1999 and 2020 in the Gulf of Taranto, corrected with geometric horizontal migration rates.

ID	Coastal Slope (degrees)	Observed Shoreline Changes (m/year)	Geometric Horizontal Migration (m/year)	Effective Shoreline Changes (m/year)
CS1	6	−0.40	−0.01	−0.39
CS2	2	−0.36	−0.03	−0.33
CS3	4	−0.38	−0.02	−0.36

5.2. Sea-Level Rise and Predicted Shoreline Positions for Two IPCC Scenarios

In order to estimate both the sea level for 2050 and 2100 AD and the subsequent sea-level rise scenario along the coast of Taranto, two regional sea-level (SL) projections, discussed in the Fifth Assessment Report of the IPCC-AR5 [23,24] and made available by the Integrated Climate data Center-ICDC of the University of Hamburg, rescaled for the Mediterranean Sea (http://icdc.cen.uni-hamburg.de/1/daten/ocean/ar5-slr.html [71]), were used. These data consist of mean values at the upper 95% and lower 5% confidence bounds of the SL, obtained by adding the contributions from geophysical sources driving long-term sea-level changes. The SL projections are based on two different Representative Concentration Pathways (RCP 2.6 and RCP 8.5), and estimated by including the thermosteric/dynamic contribution, obtained from the 21 Coupled Model Intercomparison Project Phase 5 (CMIP5). In addition, the atmosphere–ocean general circulation models (AOGCMs), the surface mass balance and dynamic ice-sheet contributions from Greenland and Antarctica, the glacier and land water storage contributions, the glacial isostatic adjustment, and the inverse barometer effect [23–25,31] were also employed. The predicted sea-level rise along the coast of Taranto was finally estimated as the sum of the above contributions and the tectonic uplift inferred from the elevation of the marine terraces of MIS 5.5 (placed at an elevation of 43 m), and the nearest Global Navigation Satellite System (GNSS) MMET stations, following the method previously applied in other areas of the Mediterranean [17,19,27,31,33,64]. The results are reported in Table 2 and Figure 17. It can be observed that both long-term and instrumental VLM rates are in agreement and provide similar mean uplift velocity of about 0.3 mm/year (MMET is uplifting at 0.29 ± 0.14 mm/year [29]; www.savemedcoasts.eu [64]), while the MIS 5.5 marine terrace provides values between 0.39 and 0.26 mm/year [40,52], supporting detailed relative sea-level (RSL) projections for 2050 and 2100.

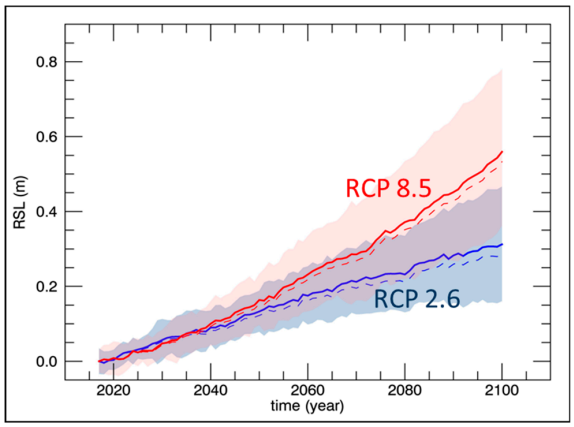

Figure 17. Graph of the sea-level rise projection estimated at the upper 95% bounds of the regional Intergovernmental Panel on Climate Change (IPCC) sea-level projections, integrated with the contribution of the mean Vertical Land Movements (VLM) rate derived from the cGPS data and long-term geological elevation of the MIS 5.5 marine terrace, relative to 2019 AD. Upper and lower curves refer to the RCP 8.5 and RCP 2.6 climate scenarios, respectively. The small scale sea-level variations are related to the modeled sea-level variability due to the ocean component contribution accounting for the effects of dynamic Sea Surface Height (SSH), the global thermosteric SSH anomaly, and the inverse barometer effects ([23,24]; http://icdc.cen.unihamburg.de/ [71]).

Table 2. Sea-level projections in the Assessment Reports 5 Representative Concentration Pathways (RCP) 2.6 and RCP 8.5 scenarios estimated for the Taranto coastal zone.

	Relative Sea-Level Rise (m)	
	2050	2100
RCP 2.6	0.133 ± 0.055	0.313 ± 0.153
RCP 8.5	0.166 ± 0.068	0.559 ± 0.209

Over the last decades, the sea-level rise in the Gulf of Taranto has been causing a generalized landward shoreline displacement and the foredune erosion, while secondary dune belts have only been partially eroded owing to the stability provided by the vegetation cover (Figure 15). With a future rise in the sea-level, the sandy coast could become extremely vulnerable due to the submersion of the entire shoreface and the marine ingression through the inlets (Figure 18).

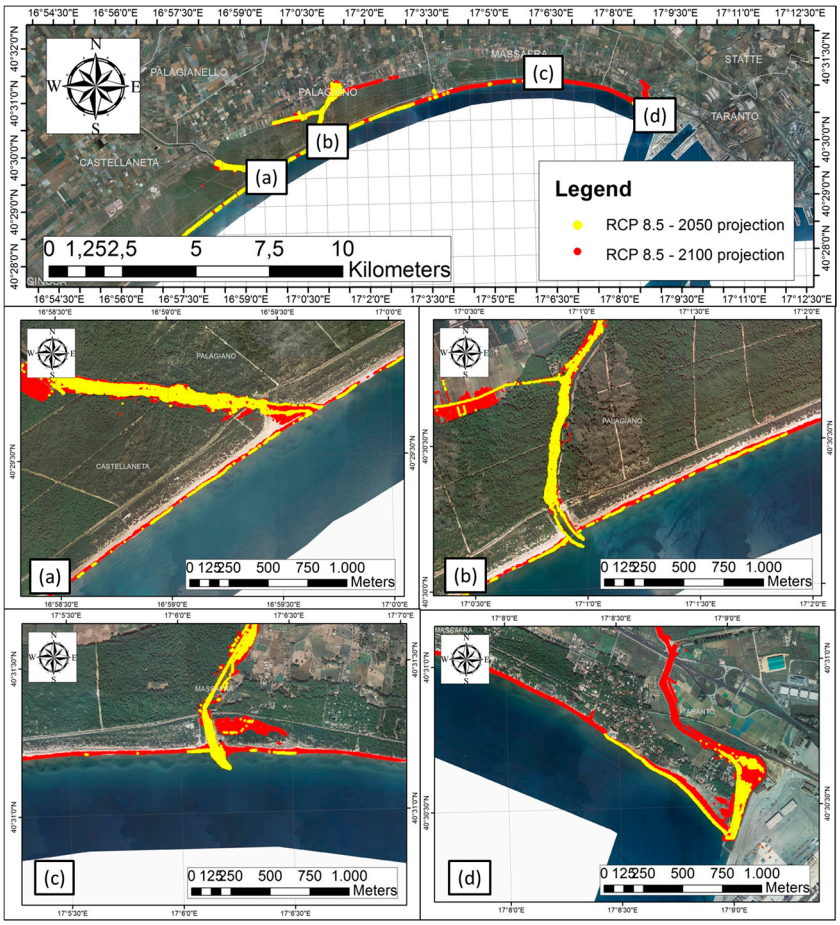

Figure 18. Submersion predictions for the coast around the Gulf of Taranto. Scenarios are relative to the AR 5 RCP 2.6 and RCP 8.5 projections of sea-level rise for 2050 and 2100 together with the VLM and horizontal displacement caused by shoreline change and sea-level rise: (**a**) the Lato River mouth; (**b**) the Lenne River mouth; (**c**) the Patemisco River mouth coastal stretch; (**d**) the Tara River mouth.

In view of a sea-level rise for 2100, the model developed in the present study describes a framework where inlets, constituted by rivers, determine preferential pathways to marine ingression. According to the Brunel and Sabatier model [9], shoreline retreats determine the destruction of the dunes during storms as some of the sand is projected behind the dunes (e.g., washover). Therefore, a shoreline retreat is accompanied by an increase in the elevation of the land behind the dunes which conditions the future position of the shoreline, and compensates, at least partially, for the sea-level rise [72]. To date,

no methodologies which include this process have been proposed. Hence, it is necessary to interpret the present results attentively. In any case, river flow regimes will certainly be affected by the increase in the sea-level and, consequently, their ability to carry sediment onto beaches will be altered.

6. Conclusions

Over the past years, the Apulian coastal systems have been subjected to relevant erosion, in part, caused by meteo-marine processes and climate changes, and, in part, by anthropogenic activities. This coastal erosion, together with sea-level rise and storm flooding, is increasing the vulnerability of the coasts.

The authors' analysis, based on available data and predictive models, enabled the reconstruction of the past dynamics of the coastal area between Castellaneta and Taranto in function of the present-day trend, as well as the development of a submersion model for future sea-level rise scenarios.

Since the mid-twentieth century, the coast has been undergoing various changes in response to sea-level rise:

- First half of the twentieth Century—progradation of the coastal system stretching from Castellaneta to Taranto, plantations of Pino d'Aleppo along the entire coast stabilized the dune system;
- 1950s–1970s—shoreline erosion highlighted along the entire littoral stretch, the building of holiday resorts in proximity to railway stations (Castellaneta Marina, Chiatona, Lido Azzurro);
- 1970s—construction of the Taranto Harbor outside the Mar Grande inlet with a substantial modification of the shoreline, and significant changes caused by the Tara, Patemisco, Lato and Lenne river mouths;
- 1970s–1990s—shoreline accretion for most of the littoral area, mainly for the beaches in proximity to the Tara river mouth, except for the Lido Azzurro and Marina di Ferrara coastal stretches, where a significant shoreline erosion and dune retreat were observed;
- 1999–2016—sea-level rise, recorded at the tide gauge in Taranto, at a rate of 1.04 ± 0.5 mm/year, and shoreline erosion recorded throughout the entire littoral area, with the exception of the area near the Tara mouth where accretion had continued;
- 2016–2018—shoreline stabilization and slow accretion in some coastal stretches, such as the Pino di Lenne beach, Chiatona beach, and Tara river mouth and an exception was made for Castellaneta, Marina di Ferrara and Lido Azzurro where a slow erosion was observed.

Considering the RCP 8.5 of sea-level projections for 2050 and 2100, together with VLM, the model output shows how open beaches will be subjected to a significant shoreline retreat with a foredune erosion and subsequent marine ingressions (Figure 18). This behavior will accelerate locally in coastal stretches already undergoing erosion, such as at Lido Azzurro and Metaponto. This will cause a complete foredune destruction with part of the sediments transported nearshore. On the other hand, adjacent to the coastal areas of Chiatona and Pino di Lenne, the model shows a significant foreshore submersion up to the dune scarp and marine ingressions through inlets of the river mouths.

Supplementary Materials: The following are available online at http://www.mdpi.com/2073-4441/12/5/1414/s1, Table S1: Images and LIDAR/TLS data used to extract the shoreline position.

Author Contributions: Conceptualization: G.S. (Giovanni Scardino), F.S., and G.M.; Data curation: G.S. (Giovanni Scardino), G.S. (Giovanni Scicchitano), F.S., M.A., A.V., and M.M.; Formal analysis: G.S. (Giovanni Scardino) and A.V.; Funding acquisition: G.M. and M.M.; Investigation: G.S. (Giovanni Scardino), F.S.; M.M., and A.P.; Methodology: G.S. (Giovanni Scardino), G.S. (Giovanni Scicchitano), F.S., M.M., A.P., and G.M.; Project administration: M.M. and A.P.; Resources: G.M., F.S., and M.M.; Software: G.S. (Giovanni Scicchitano); Visualization: M.A., F.S., and A.P.; Writing—original draft: G.S. (Giovanni Scardino), F.S., G.S. (Giovanni Scicchitano), and G.M.; Writing—review & editing: G.S. (Giovanni Scicchitano), F.S., M.A., and G.M. All authors have read and agreed to the published version of the manuscript.

Funding: This work was carried out within the Ph.D. Project of the "Programma Operativo Nazionale Ricerca e Inno-vazione 2014—2020 (CCI 2014IT16M2OP005)", Fondo Sociale Europeo, Azione I.1 "Dottorati Innovativi con caratterizzazione Industriale", Università degli Studi di Bari Aldo Moro and Integrated Sea sTORM management Stategies, Interreg ADRION European Regional Development Fund- Instrument for Pre Accession II-Fund.

Acknowledgments: We thank all those who collaborated with their logistic and technical support throughout every phase of this study. This work was carried out under the umbrella of the IGCP Project n. 639 "Sea-level change from minutes to millennia" (Project Leaders: S. Engelhart, G. Hoffmann, F. Yu and A. Rosentau) and SAVEMEDCOASTS (www.savemedcoasts.eu), funded by the European Union (DG-ECHO) (Project Coordinator Marco Anzidei). Our appreciation also goes to Victoria Sportelli, a native English speaker and lecturer, for the English language revision of the paper. We are also grateful to the reviewers for their revisions that have allowed us to improve the quality of the paper.

Conflicts of Interest: The authors declare no conflict of interest. The funders had no role in the design of the study; in the collection, analyses, or interpretation of data; in the writing of the manuscript, or in the decision to publish the results.

References

1. Aucelli, P.P.C.; Iannantuono, E.; Rosskopf, C.M. Evoluzione recente e rischio di erosione della costa molisana (*Italia meridionale*). *Ital. J. Geosci.* **2009**, *128*, 759–771. [CrossRef]
2. Aucelli, P.P.C.; Di Paola, G.; Incontri, P.; Rizzo, A.; Vilardo, G.; Benassai, G.; Buonocore, B.; Pappone, G. Coastal inundation risk assessment due to subsidence and sea level rise in a Mediterranean alluvial plain (Volturno coastal plain—Southern Italy). *Estuar. Coast. Shelf Sci.* **2017**, *198*, 597–609. [CrossRef]
3. Sabatier, F.; Samat, O.; Brunel, C.; Heurtefeux, H.; Delanghe-Sabatier, D. Determination of set-back lines on eroding coasts. Example of the beaches of the Gulf of Lions (French Mediterranean Coast). *J. Coast. Conserv.* **2009**, *13*, 57. [CrossRef]
4. Sabato, L.; Longhitano, S.G.; Gioia, D.; Cilumbriello, A.; Spalluto, L. Sedimentological and morpho-evolution maps of the 'Bosco Pantano di Policoro' coastal system (Gulf of Taranto, Southern Italy). *J. Maps* **2012**, *8*, 304–311. [CrossRef]
5. Ayadi, K.; Boutiba, M.; Sabatier, F.; Guettouche, M.S. Detection and analysis of historical variations in the shoreline, using digital aerial photos, satellite images, and topographic surveys DGPS: Case of the Bejaia bay (East Algeria). *Arab. J. Geosci.* **2015**, *9*, 26. [CrossRef]
6. Paskoff, R.P. Potential Implications of Sea-Level Rise for France. *J. Coast. Res.* **2004**, *20*, 424–434. [CrossRef]
7. Antonioli, F.; Ferranti, L.; Fontana, A.; Amorosi, A.; Bondesan, A.; Braitengerg, C.; Dutton, A.; Fontolan, G.; Furlani, S.; Lambeck, K.; et al. Holocene relative sea-level changes and vertical movements along the Italian and Istrian coastlines. *Quat. Int.* **2009**, *206*, 102–133. [CrossRef]
8. Mastronuzzi, G.; Antonioli, F.; Anzidei, M.; Auriemma, R.; Alfonso, C.; Scarano, T. Evidence of relative sea level rise along the coasts of central Apulia (Italy) during the late Holocene via maritime archaeological indicators. *Quat. Int.* **2017**, *439*, 65–78. [CrossRef]
9. Brunel, C.; Sabatier, F. Potential influence of sea-level rise in controlling shoreline position on the French Mediterranean Coast. *Geomorphology* **2009**, *107*, 47–57. [CrossRef]
10. Le Cozannet, G.; Garcin, M.; Yates, M.; Idier, D.; Meyssignac, B. Approaches to evaluate the recent impacts of sea-level rise on shoreline changes. *Earth-Sci. Rev.* **2014**, *138*, 47–60. [CrossRef]
11. Lambeck, K.; Anzidei, M.; Antonioli, F.; Benini, A.; Esposito, A. Sea level in Roman time in the Central Mediterranean and implications for recent change. *Earth Planet. Sci. Lett.* **2004**, *224*, 563–575. [CrossRef]
12. Rovere, A.; Stocchi, P.; Vacchi, M. Eustatic and Relative Sea Level Changes. *Curr. Clim. Chang. Rep.* **2016**, *2*, 221–231. [CrossRef]
13. Lambeck, K.; Antonioli, F.; Anzidei, M.; Ferranti, L.; Leoni, G.; Scicchitano, G.; Silenzi, S. Sea level change along the Italian coast during the Holocene and projections for the future. *Quat. Int.* **2011**, *232*, 250–257. [CrossRef]
14. Spampinato, C.R.; Costa, B.; Di Stefano, A.; Monaco, C.; Scicchitano, G. The contribution of tectonics to relative sea-level change during the Holocene in coastal south-eastern Sicily: New data from boreholes. *Quat. Int.* **2011**, *232*, 214–227. [CrossRef]
15. Spampinato, C.R.; Scicchitano, G.; Ferranti, L.; Monaco, C. Raised Holocene paleo-shorelines along the Capo Schisò coast, Taormina: New evidence of recent co-seismic deformation in northeastern Sicily (Italy). *J. Geodyn.* **2012**, *55*, 18–31. [CrossRef]
16. Anzidei, M.; Bosman, A.; Carluccio, R.; Casalbore, D.; Caracciolo, F.D.; Esposito, A.; Nicolosi, I.; Pietrantonio, G.; Vecchio, A.; Carmisciano, C.; et al. Flooding scenarios due to land subsidence and sea-level rise: A case study for Lipari Island (Italy). *Terra Nova* **2017**, *29*, 44–51. [CrossRef]

17. Anzidei, M.; Scicchitano, G.; Tarascio, S.; De Guidi, G.; Monaco, C.; Barreca, G.; Mazza, G.; Serpelloni, E.; Vecchio, A. Coastal retreat and marine flooding scenario for 2100: A case study along the coast of Maddalena peninsula (Southeastern Sicily). *Geogr. Fis. Din. Quat.* **2018**, *41*, 5–16. [CrossRef]
18. Anzidei, M.; Doumaz, F.; Vecchio, A.; Serpelloni, E.; Pizzimenti, L.; Civico, R.; Greco, M.; Martino, G.; Enei, F. Sea Level Rise Scenario for 2100 A.D. in the Heritage Site of Pyrgi (Santa Severa, Italy). *J. Mar. Sci. Eng.* **2020**, *8*, 64. [CrossRef]
19. Marsico, A.; Lisco, S.; Presti, V.L.; Antonioli, F.; Amorosi, A.; Anzidei, M.; Deiana, G.; Falco, G.D.; Fontana, A.; Fontolan, G.; et al. Flooding scenario for four Italian coastal plains using three relative sea level rise models. *J. Maps* **2017**, *13*, 961–967. [CrossRef]
20. Bonaldo, D.; Antonioli, F.; Archetti, R.; Bezzi, A.; Correggiari, A.; Davolio, S.; De Falco, G.; Fantini, M.; Fontolan, G.; Furlani, S.; et al. Integrating multidisciplinary instruments for assessing coastal vulnerability to erosion and sea level rise: Lessons and challenges from the Adriatic Sea, Italy. *J. Coast. Conserv.* **2019**, *23*, 19–37. [CrossRef]
21. Rahmstorf, S. A Semi-Empirical Approach to Projecting Future Sea-Level Rise. *Science* **2007**, *315*, 368–370. [CrossRef] [PubMed]
22. Rahmstorf, S.; Perrette, M.; Vermeer, M. Testing the robustness of semi-empirical sea level projections. *Clim. Dyn.* **2012**, *39*, 861–875. [CrossRef]
23. Church, J.A.; Clark, P.U.; Cazenave, A.; Gregory, J.M.; Jevrejeva, S.; Levermann, A.; Merrifield, M.A.; Milne, G.A.; Nerem, R.S.; Nunn, P.D.; et al. Sea-Level Rise by 2100. *Science* **2013**, *342*, 1445. [CrossRef] [PubMed]
24. Church, J.A.; Clark, P.U.; Cazenave, A.; Gregory, J.M.; Jevrejeva, S.; Levermann, A.; Merrifield, M.A.; Milne, G.A.; Nerem, R.S.; Nunn, P.D.; et al. Chapter 13: Sea-level change. In *Climate Change 2013: The Physical Science Basis*; Contribution of Working Group I to the Fifth Assessment Report of the Intergovernmental Panel on Climate Change; Stocker, T.F., Qin, D., Plattner, G.-K., Tignor, M., Allen, S.K., Boschung, J., Nauels, A., Xia, Y., Bex, V., Midgley, P.M., Eds.; Cambridge University Press: Cambridge, UK; New York, NY, USA, 2013; pp. 1137–1216.
25. Stocker, T.F.; Qin, D.; Plattner, G.-K.; Tignor, M.; Allen, S.K.; Boschung, J.; Nauels, A.; Xia, Y.; Bex, V.; Midgley, P.M. (Eds.) *IPCC Climate Change 2013: The Physical Science Basis*; Contribution of Working Group I to the Fifth Assessment Report of the Intergovernmental Panel on Climate Change; Cambridge University Press: Cambridge, UK; New York, NY, USA, 2013; p. 1535.
26. Pachauri, R.K.; Meyer, L.A. (Eds.) *IPCC Climate Change 2014: Synthesis Report*; Contribution of Working Groups I, II and III to the Fifth Assessment Report of the Intergovernmental Panel on Climate Change; Core Writing Team; IPCC: Geneva, Switzerland, 2014; p. 151.
27. *IPCC Special Report on the Ocean and Cryosphere in a Changing Climate*, Pörtner, H.-O.; Roberts, D.C.; Masson-Delmotte, V.; Zhai, P.; Tignor, M.; Poloczanska, E.; Mintenbeck, K.; Alegría, A.; Nicolai, M.; Okem, A.; et al. (Eds.) 2019; in press.
28. Wöppelmann, G.; Marcos, M. Coastal sea level rise in southern Europe and the nonclimate contribution of vertical land motion. *J. Geophys. Res. Ocean.* **2012**, *117*. [CrossRef]
29. Anzidei, M.; Lambeck, K.; Antonioli, F.; Furlani, S.; Mastronuzzi, G.; Serpelloni, E.; Vannucci, G. Coastal structure, sea-level changes and vertical motion of the land in the Mediterranean. *Geol. Soc. Lond. Spec. Publ.* **2014**, *388*, 453–479. [CrossRef]
30. Vermeer, M.; Rahmstorf, S. Global sea level linked to global temperature. *Proc. Natl. Acad. Sci. USA* **2009**, *106*, 21527–21532. [CrossRef]
31. Vecchio, A.; Anzidei, M.; Serpelloni, E.; Florindo, F. Natural Variability and Vertical Land Motion Contributions in the Mediterranean Sea-Level Records over the Last Two Centuries and Projections for 2100. *Water* **2019**, *11*, 1480. [CrossRef]
32. Lionello, P.; Conte, D.; Marzo, L.; Scarascia, L. The contrasting effect of increasing mean sea level and decreasing storminess on the maximum water level during storms along the coast of the Mediterranean Sea in the mid 21st century. *Glob. Planet. Chang.* **2017**, *151*, 80–91. [CrossRef]
33. Antonioli, F.; Anzidei, M.; Amorosi, A.; Lo Presti, V.; Mastronuzzi, G.; Deiana, G.; De Falco, G.; Fontana, A.; Fontolan, G.; Lisco, S.; et al. Sea-level rise and potential drowning of the Italian coastal plains: Flooding risk scenarios for 2100. *Quat. Sci. Rev.* **2017**, *158*, 29–43. [CrossRef]

34. Bamber, J.L.; Oppenheimer, M.; Kopp, R.E.; Aspinall, W.P.; Cooke, R.M. Ice sheet contributions to future sea-level rise from structured expert judgment. *Proc. Natl. Acad. Sci. USA* **2019**, *116*, 11195–11200. [CrossRef]
35. Kulp, S.A.; Strauss, B.H. New elevation data triple estimates of global vulnerability to sea-level rise and coastal flooding. *Nat. Commun.* **2019**, *10*, 1–12. [CrossRef]
36. Mastronuzzi, G.; Aringoli, D.; Aucelli, P.P.C.; Baldassarre, M.A.; Bellotti, P.; Bini, M.; Biolchi, S.; Bontempi, S.; Brandolini, P.; Chelli, A.; et al. Geomorphological map of the Italian Coast: From a descriptive to a morphodynamic approach. *Geogr. Fis. Din. Quat.* **2017**, *40*, 161–195. [CrossRef]
37. Carbognin, L.; Teatini, P.; Tosi, L. Eustacy and land subsidence in the Venice Lagoon at the beginning of the new millennium. *J. Mar. Syst.* **2004**, *51*, 345–353. [CrossRef]
38. Caldara, M.; Capolongo, D.; Damato, B.; Pennetta, L. Can the ground laser scanning technology be useful for coastal defenses monitoring? *Ital. J. Eng. Geol. Environ.* **2006**, *1*, 35–49.
39. Syvitski, J.P.M.; Kettner, A.J.; Overeem, I.; Hutton, E.W.H.; Hannon, M.T.; Brakenridge, G.R.; Day, J.; Vörösmarty, C.; Saito, Y.; Giosan, L.; et al. Sinking deltas due to human activities. *Nat. Geosci.* **2009**, *2*, 681–686. [CrossRef]
40. De Santis, V.; Caldara, M.; Torres, T.; Ortiz, J.E.; Sánchez-Palencia, Y. A review of MIS 7 and MIS 5 terrace deposits along the Gulf of Taranto based on new stratigraphic and chronological data. *Ital. J. Geosci.* **2018**, *137*, 349–368. [CrossRef]
41. Bruun, P. Sea-Level Rise as a Cause of Shore Erosion. *J. Waterw. Harb. Div.* **1962**, *88*, 117–132.
42. Dubois, R.N. How does a Barrier Shoreface Respond to a Sea-Level Rise? *J. Coast. Res.* **2002**, *18*, 3–5.
43. Lorenzo-Trueba, J.; Ashton, A.D. Rollover, drowning, and discontinuous retreat: Distinct modes of barrier response to sea-level rise arising from a simple morphodynamic model. *J. Geophys. Res. Earth Surf.* **2014**, *119*, 779–801. [CrossRef]
44. Valentin, H. Die Küsten der Erde. *Petermanns Geogr. Mitt. Ergänzsungheft* **1952**, *246*, 118.
45. Wong, T.E.; Bakker, A.M.; Keller, K. Impacts of Antarctic fast dynamics on sea level projections and coastal flood defense. *Clim. Change* **2017**, *144*, 347–364. [CrossRef]
46. Bruun, P. *Coast Erosion and the Development of Beach Profiles*; U.S. Beach Erosion Board: Washington, DC, USA, 1954.
47. Davidson-Arnott, R.G.D. Conceptual Model of the Effects of Sea Level Rise on Sandy Coasts. *J. Coast. Res.* **2005**, *21*, 1166–1172. [CrossRef]
48. Cilumbriello, A.; Sabato, L.; Tropeano, M.; Gallicchio, S.; Grippa, A.; Maiorano, P.; Mateu-Vicens, G.; Rossi, C.A.; Spilotro, G.; Calcagnile, L.; et al. Sedimentology, stratigraphic architecture and preliminary hydrostratigraphy of the Metaponto coastal-plain subsurface (Southern Italy). *Mem. Descr. Carta Geol. d'Ital.* **2010**, *XC*, 67–84.
49. Tropeano, M.; Cilumbriello, A.; Sabato, L.; Gallicchio, S.; Grippa, A.; Longhitano, S.G.; Bianca, M.; Gallipoli, M.R.; Mucciarelli, M.; Spilotro, G. Surface and subsurface of the Metaponto Coastal Plain (Gulf of Taranto—Southern Italy): Present-day- vs. LGM-landscape. *Geomorphology* **2013**, *203*, 115–131. [CrossRef]
50. Nakada, M.; Lambeck, K. The melting history of the late Pleistocene Antarctic ice sheet. *Nature* **1988**, *333*, 36–40. [CrossRef]
51. Mastronuzzi, G.; Sansò, P. Morfologia e genesi delle Isole Chéradi e del Mar Grande (Taranto, Puglia, Italia). *Geogr. Fis. Din. Quat.* **1998**, *21*, 131–138.
52. Mastronuzzi, G.; Sansò, P. Quaternary coastal morphology and sea level changes. In *Proceedings of the Puglia 2003, Final Conference—Project IGCP 437 UNESCO—IUGS, Otranto/Taranto, Puglia, Italy, 22–28 September 2003*; GIS Coast Coast—Gruppo Informale di Studi Costieri, Research Publication: Taranto, Italy, 2003; Volume 5, p. 184.
53. Valenzano, E.; Scardino, G.; Cipriano, G.; Fago, P.; Capolongo, D.; De Giosa, F.; Lisco, S.; Mele, D.; Moretti, M.; Mastronuzzi, G. Holocene Morpho-Sedimentary Evolution of the Mar Piccolo Basin (Taranto, Southern Italy). *Geogr. Fis. Din. Quat.* **2018**, *41*, 119–135. [CrossRef]
54. Zander, A.; Fulling, A.; Brückner, H.; Mastronuzzi, G. OSL dating of upper pleistocene littoral sediments: A contribution to the chronostratigraphy of raised marine terraces bordering the Gulf of Taranto, South Italy. *Geogr. Fis. Din. Quat.* **2006**, *29*, 33–50.
55. Carter, R.W.G. *Coastal Evolution: Late Quaternary Shoreline Morphodynamics*; Reprint Edizione; Cambridge University Press: Cambridge, UK, 1997; ISBN 978-0-521-59890-3.

56. Mastronuzzi, G.; Sansò, P. Pleistocene sea-level changes, sapping processes and development of valley networks in the Apulia region (Southern Italy). *Geomorphology* **2002**, *46*, 19–34. [CrossRef]
57. Mastronuzzi, G.; Romaniello, L. Holocene aeolian morphogenetic phases in Southern Italy: Problems in 14C age determinations using terrestrial gastropods. *Quat. Int.* **2008**, *183*, 123–134. [CrossRef]
58. Caldara, M.; Centenaro, E.; Mastronuzzi, G.; Sansò, P.; Sergio, A. Features and present evolution of Apulian Coast (Southern Italy). *J. Coast. Res.* **1998**, *SI*, 55–64.
59. Lisi, I.; Bruschi, A.; Del Gizzo, M.; Archina, M.; Barbano, A.; Corsini, S. Le unità fisiografiche e le profondità di chiusura della costa italiana. *L'ACQUA* **2010**, *2*, 35–52.
60. Di Bucci, D.; Caputo, R.; Mastronuzzi, G.; Fracassi, U.; Selleri, G.; Sansò, P. Quantitative analysis of extensional joints in the Southern Adriatic foreland (Italy), and the active tectonics of the Apulia region. *J. Geodyn.* **2011**, *51*, 141–155. [CrossRef]
61. Amorosi, A.; Antonioli, F.; Bertini, A.; Marabini, S.; Mastronuzzi, G.; Montagna, P.; Negri, A.; Rossi, V.; Scarponi, D.; Taviani, M.; et al. The Middle–Upper Pleistocene Fronte Section (Taranto, Italy): An exceptionally preserved marine record of the Last Interglacial. *Glob. Planet. Chang.* **2014**, *119*, 23–38. [CrossRef]
62. Lisco, S.; Corselli, C.; De Giosa, F.; Mastronuzzi, G.; Moretti, M.; Siniscalchi, A.; Marchese, F.; Bracchi, V.; Tessarolo, C.; Tursi, A. Geology of Mar Piccolo, Taranto (Southern Italy): The physical basis for remediation of a polluted marine area. *J. Maps* **2016**, *12*, 173–180. [CrossRef]
63. Polcari, M.; Albano, M.; Montuori, A.; Bignami, C.; Tolomei, C.; Pezzo, G.; Falcone, S.; La Piana, C.; Doumaz, F.; Salvi, S.; et al. InSAR Monitoring of Italian Coastline Revealing Natural and Anthropogenic Ground Deformation Phenomena and Future Perspectives. *Sustainability* **2018**, *10*, 3152. [CrossRef]
64. Savemedcoasts. Available online: http://www.savemedcoasts.eu/ (accessed on 4 April 2020).
65. RING—Rete Integrata Nazionale GPS. Available online: http://ring.gm.ingv.it/ (accessed on 25 April 2020).
66. Altamimi, Z.; Collilieux, X.; Métivier, L. ITRF2008: An improved solution of the international terrestrial reference frame. *J. Geod.* **2011**, *85*, 457–473. [CrossRef]
67. Rete Mareografica Nazionale—Homepage. Available online: https://mareografico.it/ (accessed on 4 April 2020).
68. Attivazione Del Nuovo Sistema Informativo Meteo Oceanografico Delle Coste Pugliesi (Simop). Available online: https://www.adb.puglia.it/public/news.php?extend.282 (accessed on 4 April 2020).
69. Theiler, E.; Himmelstoss, E.; Zichichi, J.; Ergul, A. *Digital Shoreline Analysis System (DSAS) Version 4.0-An ArcGIS Extension for Calculating Shoreline Change (Ver. 4.4, July 2017)*; U.S. Geological Survey Open-File Report; USGS, U.S.: Reston, VA, USA, 2017; p. 1278.
70. Bonora, N.; Immordino, F.; Schiavi, C.; Simeoni, U.; Valpreda, E. Interaction between Catchment Basin Management and Coastal Evolution (Southern Italy). *J. Coast. Res.* **2002**, 81–88. [CrossRef]
71. AR5 Sea Level Rise. Available online: http://icdc.cen.uni-hamburg.de/1/daten/ocean/ar5-slr.html (accessed on 25 April 2020).
72. Sabatier, F.; Provansal, M.; Fleury, T.-J. Discussion of: PASKOFF, R., 2004. Potential Implications of Sea-Level Rise for France. *J. Coast. Res.* **2004**, *20*, 424–434. [CrossRef]